

Supporting Information

Molecular docking-assisted design and synthesis of an anti-tumor quercetin-Se(IV) complex

Xu Chen,^{ab} Xianyong Wu,^a Ziyu He,^a Juan Zhang,^a Ya Cao,^a Dongsheng Mao,^a Chang Feng,^a Bo Tian*^a and Guifang Chen*^a

^a Center for Molecular Recognition and Biosensing, School of Life Sciences, Shanghai University, Shanghai, PR China

^b Experimental Center for Life Sciences, Shanghai University, Shanghai, PR China

*Corresponding authors. E-mail addresses: gfchen@shu.edu.cn (G. Chen); botian@shu.edu.cn (B. Tian).

Table of Contents	page
Figure S1: UV-vis spectrum of QUE and QUE-Se	2
Figure S2: IR Spectrum of QUE and QUE-Se	3
Figure S3: ¹ H NMR (600 M) of QUE-Se and QUE in DMSO	4
Figure S4: ESI-MS spectra of QUE-Se and its calculated isotopic pattern	5
Figure S5: 3D fluorescence spectra of QUE and QUE-Se	6
Figure S6: HPLC-FL chromatograms of QUE and QUE-Se in the absence and presence of DMEM medium	7
Figure S7: The activity of selenium dioxide	8
Figure S8: Plot of change relative specific viscosity of CT-DNA with increasing concentration of QUE and QUE-Se	9

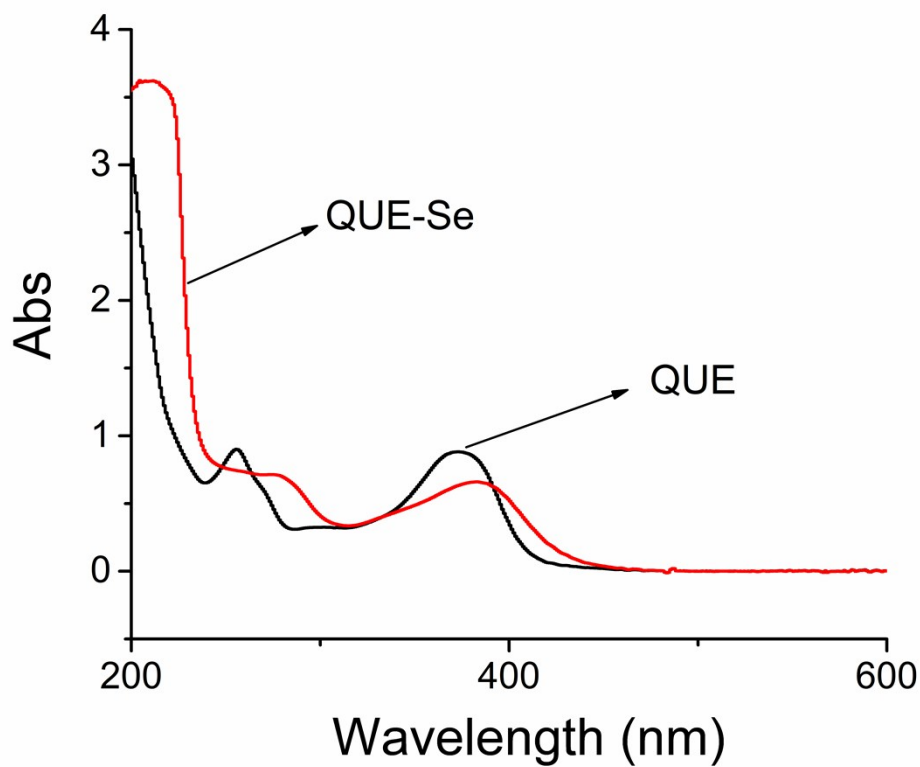


Fig. S1. UV-vis spectrum of QUE and QUE-Se.

UV-vis spectra were recorded on Varian Cary 100 instrument. The absorption peak of QUE at 255 nm was caused by the electronic transition of the benzoyl group of the A ring, and at 372 nm due to the electronic transition of the cinnamoyl group of the B ring. The UV-visible spectrum analysis of QUE-Se showed significant shifts on both peaks, indicating that the structure of QUE-Se changed compared with quercetin.

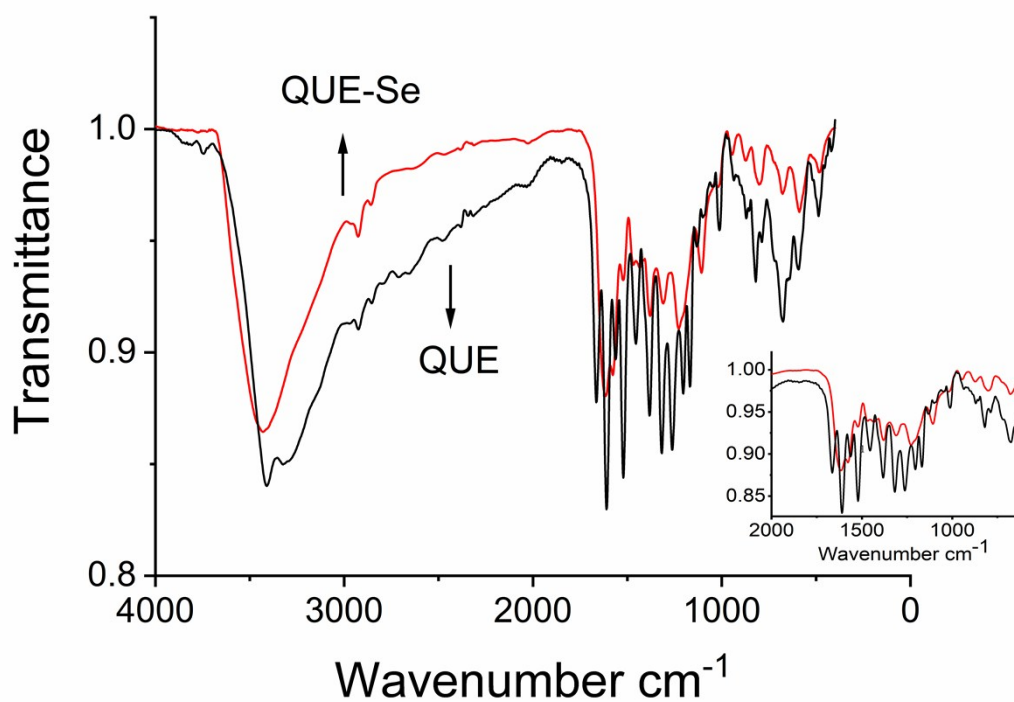


Fig. S2. IR Spectrum of QUE and QUE-Se.

IR spectra were recorded on Bruker VERTEX70 instrument. The 1665 cm⁻¹ absorption peak strength of C=O bond stretching vibration in quercetin was obviously shifted to the low wavenumber direction, and it was speculated that C=O bond of quercetin was involved in Se(IV) coordination.

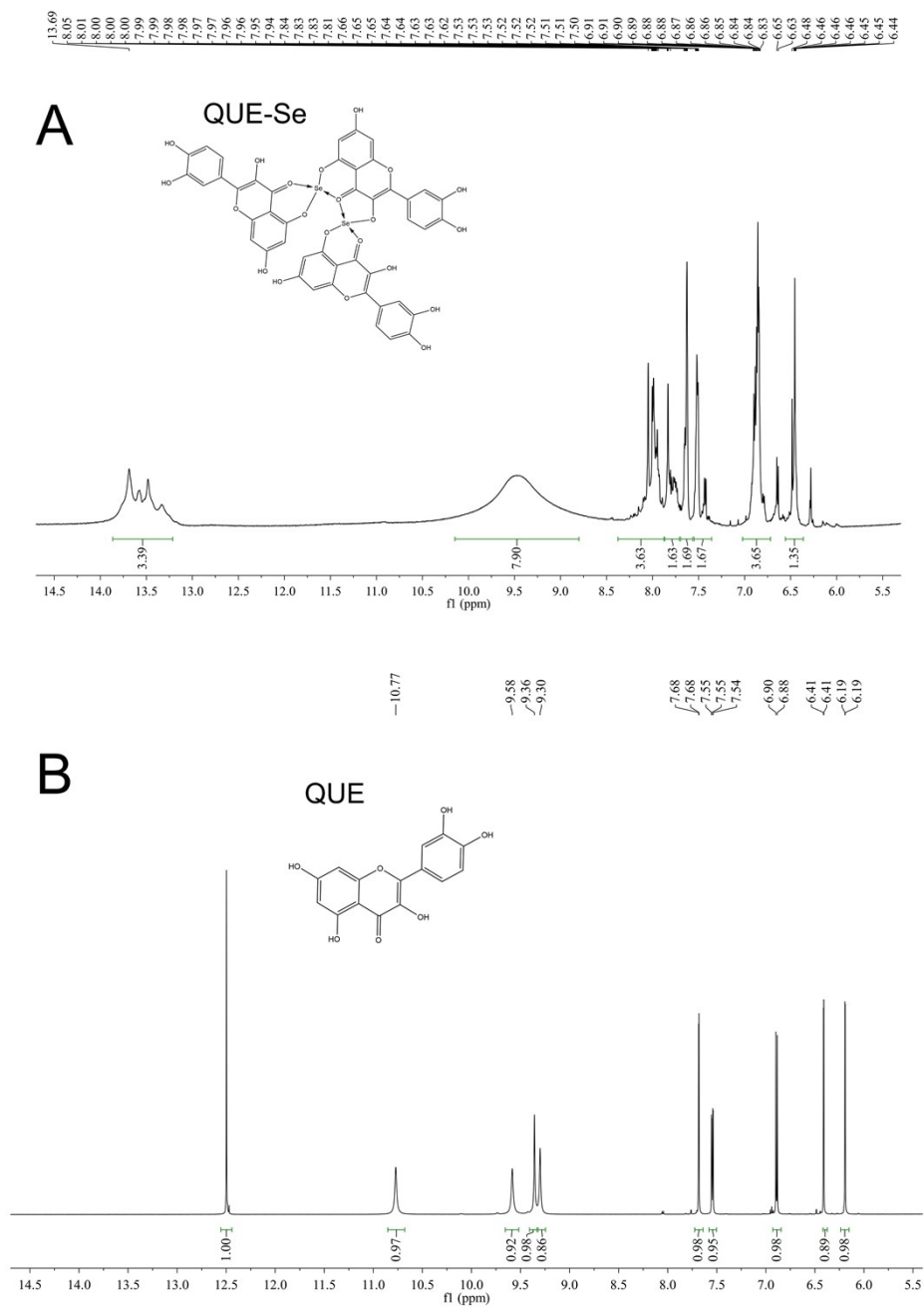


Fig. S3. ^1H NMR (600 M) of QUE-Se and QUE in DMSO.

(A) QUE-Se ^1H NMR (600 MHz, DMSO) δ 13.69–13.30 (m, 3H), 9.47 (s, 8H), 8.05–7.92 (m, 4H), 7.84–7.73 (m, 2H), 7.66–7.62 (m, 2H), 7.54–7.38 (m, 2H), 6.94–6.79 (m, 4H), 6.48–6.43 (m, 1H). (B) QUE ^1H NMR (600 MHz, DMSO- d_6) δ 12.50 (s, 1H), 10.77 (s, 1H), 9.58 (s, 1H), 9.36 (s, 1H), 9.30 (s, 1H), 7.68 (d, $J = 2.2$ Hz, 1H), 7.58–7.50 (m, 1H), 6.89 (d, $J = 8.5$ Hz, 1H), 6.41 (d, $J = 2.0$ Hz, 1H), 6.19 (d, $J = 2.0$ Hz, 1H). ^1H NMR spectra were recorded on Bruker AVANCE III HD 600MHz.

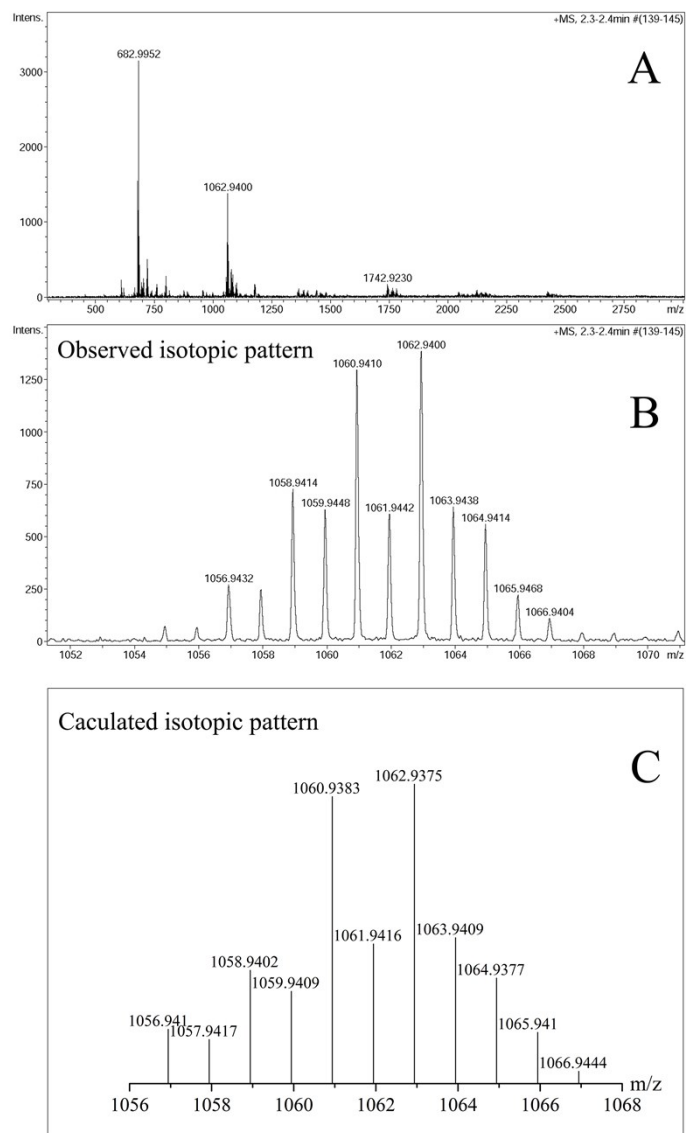


Fig. S4. ESI-MS spectra of QUE-Se and its calculated isotopic pattern ($C_{45}H_{26}O_{21}Se_2$) : 1062.9400 $[M+H]^+$

(A) Positive ESI-MS spectra of QUE-Se. (B) Observed isotopic pattern. (C) Calculated isotopic pattern. Mass spectra were measured on Bruker MicroTOF. QUE-Se easily lost one molecule of quercetin and selenium, separated into fragment ions 682.9952 $[M+H]^+$.

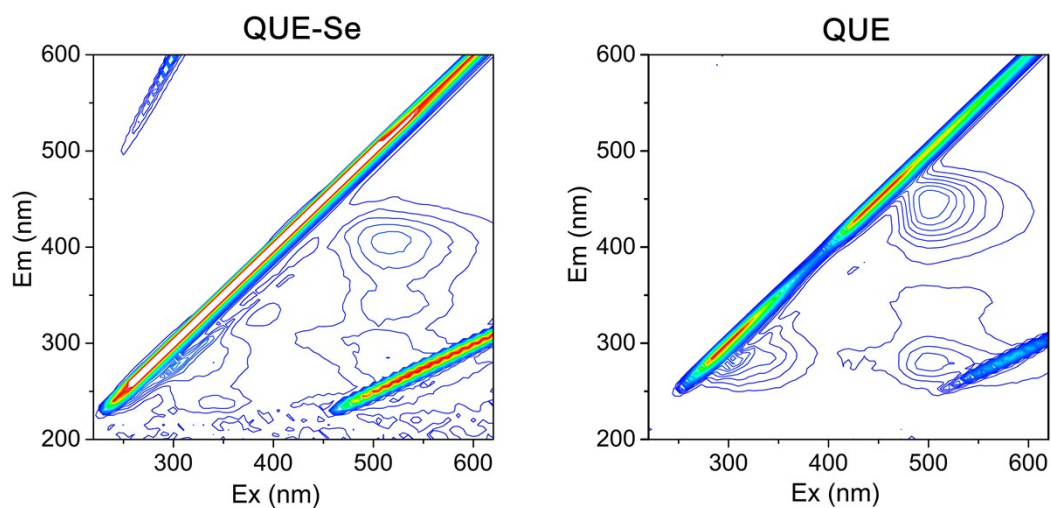


Fig. S5. 3D fluorescence spectra of quercetin (QUE) and QUE-Se.

The 3D fluorescence spectra of QUE-Se and QUE were recorded at the same concentration 1.35 mg/mL on Hitachi F-7000 apparatus. QUE-Se (Ex/Em: 410/530 nm), QUE (Ex/Em: 430/490 nm).

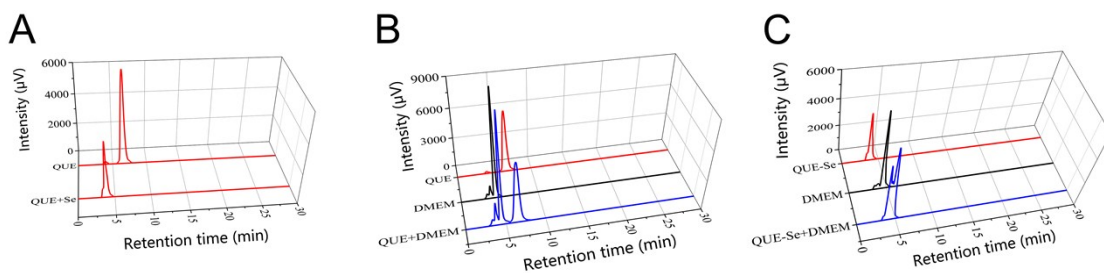


Fig. S6. HPLC-FL chromatograms of QUE and QUE-Se in the absence and presence of DMEM medium.

(A) HPLC chromatograms of QUE and QUE-Se in the absence of DMEM medium. (B) HPLC chromatograms of QUE in the presence of DMEM medium. (C) HPLC chromatograms of QUE-Se in the presence of DMEM medium.

HPLC-FL analysis was performed in Shimadzu LC-20A coupled to a fluorescence detector (RF-20A) using a 5 μm C_{18} column (250 \times 4.6 mm I.D). The column was operated at 40 $^{\circ}\text{C}$. The mobile phase consisted of 70 % (v/v) methanol in water. The fluorescence detector was set at 430/490 nm for QUE detection and 410/530 nm for QUE-Se detection. The injection volume was 10 μL . The flow-rate was at 0.7 mL/min. QUE and QUE-Se were prepared at the same concentration 1.35 mg/mL. The compounds in absence of DMEM medium were precipitated by methanol and centrifugated for 5 min (10000 r/min). QUE and QUE-Se were stable in 3 days. It could be found that QUE and QUE-Se had good chemical stability in culture medium.

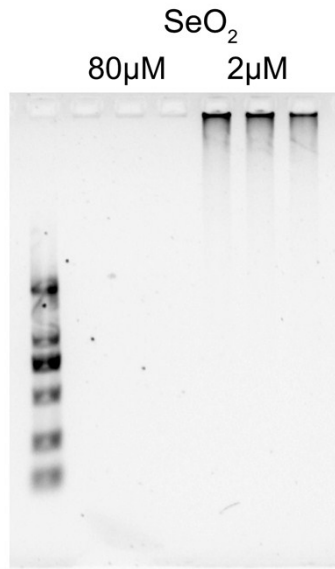


Fig. S7. The activity of selenium dioxide. No significant inhibitory of SeO₂ (2 μM) on DNA amplification.

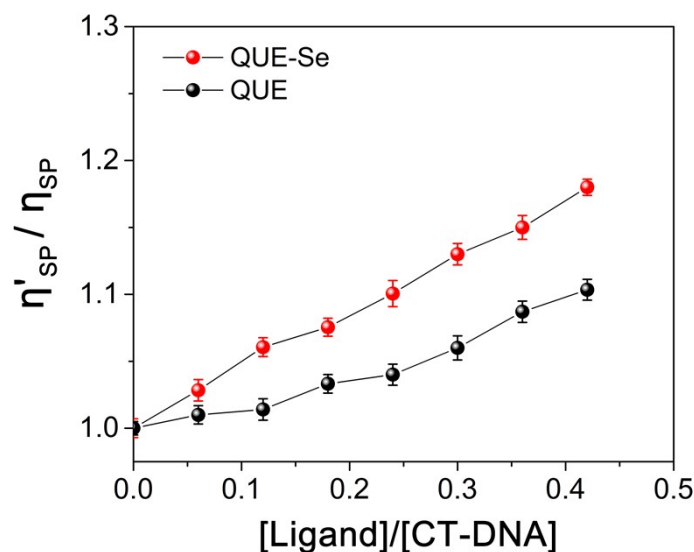


Fig. S8. Plot of change relative specific viscosity of CT-DNA with increasing concentration of QUE and QUE-Se. The concentration of CT-DNA was 500 μ M.

The viscometry measurements were performed on a Discovery HR-3 Hybrid Rheometer (TA Instruments, New Caste, USA) maintained at 25 ± 0.5 °C. The experiments were carried out by keeping the DNA concentration while increasing concentration of QUE and QUE-Se to give a certain r ($r = [\text{Ligand}]/[\text{CT-DNA}]$) value. The relative viscosity data were represented as η'_{sp}/η_{sp} versus the $[\text{Ligand}]/[\text{CT-DNA}]$ ratio r , where η_{sp} is the viscosity of ligand treated DNA, η'_{sp} is the viscosity of untreated DNA.

To further verify the binding mode of QUE and QUE-Se with DNA, the viscometric study was employed. Viscosity is sensitive to DNA-length changes. In case of intercalation binding, small molecules induce extension and unwinding of the DNA backbone due to separation of base pairs, which can lead to an increase in the viscosity of DNA. In contrast, groove binding agents cause little or no diatortion to the DNA backbone and thereby have little effect on the viscosity of DNA. Figure S8 represented the effect of QUE and QUE-Se on the viscosity of CT-DNA solution. The gradual enhancement in the relative viscosity value of DNA in presence of QUE and QUE-Se confirmed the intercalation binding mode. There were more significant changes in case of QUE-SE complex bound to DNA. The results were consistent with CD results.